Title
A Study on the Functional Role of Hsp90α in Head and Neck Cancer Invasion

Author
ELZAKRA, NASEIM

Publication Date
2015

Peer reviewed|Thesis/dissertation

UNIVERSITY OF CALIFORNIA

Los Angeles

A Study on the Potential Role of Hsp90α in Head and Neck Cancer Invasion

A thesis submitted in partial satisfaction of the requirements of the degree Master of Science in Oral Biology

By

Naseim Elzakra

2015

ABSTRACT OF THE THESIS

A Study on the Functional Role of Hsp90α in Head and Neck Cancer Invasion

By

Naseim Elzakra

Master of Science in Oral Biology

University of California, Los Angeles, 2015

Professor Shen Hu, Chair

Background: Many cellular processes are involved in maintaining the cancer microenvironment. Hsp90α is up-regulated in a number of different cancer tissues including breast cancer, prostate cancer, small cell lung cancer, acute myeloid leukemia among others, and it has been regarded as a potent cancer biomarker through stabilizing the oncogenic proteins integrity and functionally. Previous studies showed that Hsp90α inhibition reduces many key oncogenic proteins

responsible for cancer signaling, proliferation, invasion and survival. Therefore, identifying a potential role of Hsp90 in the head and neck squamous cell carcinoma phenotype followed with identifying Hsp90α client proteins is a rational approach to further understand the underlying process of head and neck squamous cell carcinoma (HNSCC). A preliminary study conducted in our lab showed the transcription factor SOX11 to be up-regulated in the highly invasive HNSCC cancer cell lines versus low invasive ones, through which we hypothesized that SOX11 might be a potential new client protein for Hsp90α.

Objective: To study the functional role of Hsp90α in the invasiveness, motility and survival of the HNSCC cells and to discover a new client protein to further understand the mechanism and mode of action of the Hsp90α in HNSCC cell lines.

Aim #1: To analyze and compare the expression of the cytoplasmic and membranous Hsp90α among different HNSCC cell lines.

Aim #2: To identify the functional role of Hsp90α on the phenotypic traits of the invasive HNSCC cells.

Aim #3: To identify the functional biochemical interaction between Hsp90α as a chaperone and SOX11 as a potential client protein.

Aim #4: To determine a potential SOX11 up-stream regulatory role on Hsp90α.

Materials and Methods: Western Blotting and qPCR were used to assess the expression of Hsp90α among four HNSCC cell lines, UM1, UM2, UM5 and UM6. Phenotypic studies including proliferation, migration and invasion assays were performed after a siRNA knockdown

of Hsp90α to investigate the functional role of Hsp90α in HNSCC cells. We performed a Co-IP assay using SOX11 antibody to pull down SOX11 and its associated proteins on a proteomic scale and use liquid chromatography mass spectrometry (LC-MS/MS) to identify the binding proteins that have possible functional interaction with SOX11. A Co-IP experiment using SOX11 antibody followed by Western blot analysis of Hsp90α was used to confirm the MS results, and a second Co-IP experiment using Hsp90α antibody followed with Western blot analysis of SOX11 was conducted to further confirm the binding between Hsp90α and SOX11. siRNA knock down of SOX11 was performed to assess if down-regulation of SOX11 affects the expression of Hsp90α in HNSCC cells.

Result: Both Western blotting and qPCR indicated that Hsp90α is over-expressed in the invasive UM1 and UM5 cell lines when compared to low invasive UM2 and UM6 cell lines ($p<0.05$). Hsp90α transient knock down in highly invasive UM1 and UM5 cell lines to assess the role of Hsp90α on proliferation, migration and invasion resulted in a proliferation assay showing a declined proliferation course in the knockdown set ($p < 0.05$). Wound healing assay showed a 40% decrease in UM1 migration potency ($p < 0.001$). *Similarly,* invasion assay showed 99% (UM1) and 89.2% (UM5) decrease in invasion potential ($p < 0.001$). *LC-MS/*MS analysis of the Co-IP samples of UM1 and UM5 cell lines showed that Hsp90α is among the high abundant proteins that binds to SOX11. The MS data was confirmed by a Co-IP assay using SOX11 antibody followed by Western blot analysis of Hsp90α, which shows the potential binding between SOX11 and Hsp90α. The second Co-IP assay conducted using Hsp90α antibody and Western blot analysis of SOX11 also confirmed the binding between the two proteins. Finally,

After the knockdown of SOX11 in UM1 and UM5 cells with siRNA, there was no significant reduction of Hsp90α levels.

Conclusion: Hsp90α may play an important functional role in the invasiveness of HNSCC cells. SOX11 could be a potential client protein for Hsp90α. the transcriptional factor SOX11 may not directly regulate the expression of Hsp90.

The thesis of Naseim Elzakra is approved.

Robert Chiu

Renate Lux

Richard G. Stevenson

Shen Hu, Committee Chair

University of California, Los Angeles

2015

DEDICATION

I dedicate this humble work to my family and my mentor Dr. Shen Hu.

TABLE OF CONTENTS

ABSTRACT OF THESIS……ii

DEDICATION……..…….…….vii

TABLE OF CONTENTS…….…..……viii

LIST OF FIGURES AND TABLES ……..….ix

INTRODUCTION……..…….……..1

MATERIALS AND METHODS….…….……5

RESULTS……..…….……..……12

DISCUSSION……..…….……..……15

CONCLUSION…..……..17

FIGURES AND TABLES……..…….18

REFERENCES……33

LIST OF FIGURES AND TABLES

FIGURE 1: ……..……..19

FIGURE 2: ……..……..20

FIGURE 3: ……..……..21

FIGURE 4: ……..……..22

FIGURE 5: ……..……..23

FIGURE 6: ……..……..24

FIGURE 7: ……..……..25

FIGURE 8: ……..……..26

FIGURE 9: ……..……..27

FIGURE 10: ……..……..28

FIGURE 11 ……..……..29

FIGURE 12 ……..……..30

FIGURE 13 ……..……..……..31

TABLE 1: Primers ……..…….32

INTRODUCTION

HNSCC

Head and Neck squamous cell carcinoma (HNSCC) is considered as the sixth most common cancer and also the most common tumor type in the head and neck region. Worldwide the disease affects 640,000 new patients each year, and there is an estimate of 50,000 new cases and 10,000 deaths from HNSCC have been recorded in the United states annually [1] [2]. The 5-year survival rate is approximately 50% and has decreased only minimally during the last decades.

The anatomical heterogeneity of HNSCC complicate their consideration as a single disease entity. Oral squamous cell carcinoma (OSCC) is a main subtype of HNSCC. The highest incidence of oral squamous cell carcinoma (OSCC) rates are found in South-Central Asia, Eastern and Central Europe and the lowest being in Africa, Central America, and Eastern Asia for both males and females **(Figure. 1)**. The most important risk factors are tobacco use, alcohol consumption, with smoking and alcohol having synergistic effects [3]. High-risk human papilloma viruses (HPV) types play a major role in oropharynx cancer [4], whereas Barr virus accounts for the majority of nasopharyngeal cancer (NPCs) [5]. Other notable factors include chewing betel nut, poor oral hygiene, exposure to carcinogenic chemicals, and possibly infection with human immunodeficiency virus. Almost 60% of patients are presented with an advanced presentation of the lesion at the time of diagnosis, for the reason that HNSCC tumors are often asymptomatic in the early stages. Treatment for HNSCC has been recently shifting from the empirical treatment modalities such as surgery, radiotherapy, chemotherapy to a target-specific

treatment. Although, many target-specific anti-cancer therapies have been developed, patient survival has not been improved as patients still develop recurrence, distant metastasis, and secondary primary tumors [6]. Therefore, it is imperative for new biomarkers to be established to help with the early detection, prognosis and treatment of HNSCC as no prognostic biomarker in the HNSCC has yet been able to provide means to predict the treatment modalities used to counteract the oncogenic process. In contrast, other tumor types have shown targetable signaling pathways and specific genomic transformation accordant to treatment outcomes.

HSPs/ Hsp90α

Heat shock proteins (HSPs) are chaperones responsible for the heat shock response (HSR). HSR first discovered by Ferruccio Ritossa in 1962 [7], is an arranged genetic reaction to varied environmental and physiological stressors that resuLts in the activation of genes encoding molecular chaperones for a recovery from cellular damage associated with the expression of mis-folded proteins [7]. Those stress-inducers include acute and chronic conditions such as elevated temperatures, chemical toxicants, infection, and oxidative stress. Mutations and environmental influences including inflammation, ischemia, tissue wounding and repair, cancer, and neurodegenerative diseases are also associated with the aberrant expression of HSPs [8]. The heat shock gene superfamily is classified by molecular size into Hsp100, Hsp90, Hsp70, Hsp60 and the small HSPs [9], and their function is to assist proper protein folding and prevent aggregation of non-native proteins [10]. Hsp90α is a highly abundant protein, constituting about 1–2% of total proteins in non-stressed tissues and about 4-6% in stressed tissues [11]. Through the application of global analysis techniques, more than 200 proteins had been identified as client

protein for Hsp90α [12][13][14]. Under normal non-stress conditions, Hsp90α plays a major role for normal cell viability and growth [15]. During environmental stress, Hsp90α is required for the cell cycle, meiosis, and cellular trafficking [16]. Hsp90α exists as a dimer, each monomer consisting of three highly conserved domains: an N-terminal ATP-binding domain, a middle domain where the client proteins bind and a C-terminal dimerization domain [17] **(Figure. 2)**. The open state of the two N-terminal Hsp90α dimer can bind to client proteins [18], followed with ATP binding that leads to the formation of the closed state to clamp client proteins inside [18][19]. The Hsp90α inhibitors result in disruption of the Hsp90α functional configuration leading to degradation of Hsp90α client proteins by the ubiquitin-dependent proteasome pathway [20]. In view of the observation that Hsp90α inhibitors bear potent anti-cancer effect [21][22], Hp90 has become validated as a potential target in cancer therapy. Furthermore, preclinical and clinical evaluation of a wide array of Hsp90α inhibitors has already shown promising results as a single agent and/or in combination with chemotherapy.

Hsp90α and the main client proteins

In eukaryotic cells, the two major isoforms of Hsp90 are Hsp90α and Hsp90β, which are encoded by two distinct genes, share approximately 81% sequence homology. Hsp90α had been long considered a cytoplasm protein. However, a pool of Hsp90α has been described to be an *extra*cellular protein, which was associated with tumor cell invasion through serving as a molecular chaperone of matrix metalloprotease 2 (MMP-2), an extracellular enzyme essential for cell invasion [23]. Additionally, Hsp90α is important for cell motility through assisting the maturity of Her-2 [24]. Hsp90α is known to stabilize both wild type and mutant EGFR, a

tyrosine kinase responsible for the uncontrolled cell division in cancer [22]. Inhibition of the Hsp90α in turns down-regulated HIF-1α and NF-κB and resulted in inhibition of epithelial to mesenchymal transition (EMT), invasion, and motility of cancer cell lines [21].

SOX11

The SOX protein family of transcription factors is considered as regulators during embryonic development, cell-fate decisions and lineage commitment, determination and differentiation [25]. SOX11, a member of the SOX family, plays an important role in both embryonic and adult neurogenesis[26]. SOX11 up-regulation has been detected in various types of solid tumors, such as gliomas [27], gastric cancer [28], mantle cell lymphoma [29]and epithelial ovarian tumors[30] . SOX11 has been considered a diagnostic biomarker for many solid tumors [30]. However, the specific role of SOX11 in HNSCC has not been understood yet.

MATERIALS AND METHODS

Cell Culture

The oral/head and neck squamous cell carcinoma cell lines, UM1, UM2, UM5, and UM6 cell lines, were obtained from Dr. Yong Kim at the UCLA School of Dentistry. All cell lines were cultured in DMEM with 10% fetal bovine serum, 100-units/ml penicillin G and 100 μg/mL streptomycin. Normal human oral keratinocytes (NHOK) were cultured in keratinocyte basal media containing keratinocyte growth factors. Cell cultures were maintained in a humidified atmosphere of 5% CO_2, 95% air at 37 °C. Cell culture medium was changed every two days.

Western blotting

At 80% confluence in 10 cm plate of UM1, UM2, UM5, UM6 and NHOK cell lines were lysed using Rehydration Buffer (RB) containing 7M Urea, 2M Thiourea, 50mM DTT, 4%CHAPS, 5%Glycerol, 10%Isopropanol and 70% /(V/V) H2O. The cell lysates were centrifuged at 14,000 rpm for 5 minutes at 4°C. The supernatants were removed and the total concentration of proteins were quantified using micro BCA assay at 595 nM. Afterwards, 15ug of cell lysate were loaded onto NUPAGE Novex 4-12% Bis-Tris gels to separate the proteins along with 7μl protein marker. The Gel running setting was adjusted at 120 V for 2 hours using running buffer of MOP (Tris base, MOP, SDS, EDTA, H2O). The gel was then transferred to a Nitrocellulose membrane in transfer buffer at 15 V for 45 minutes at room temperature. The membrane was cut into two pieces (one for Hsp90α and the other for GAPDH). Blocking both membranes with 5% milk in TBST with 10% Tween20 for one hour at room temperature was

followed before adding Hsp90α polyclonal antibodies (SANTA CRUZ) at a dilution of 1:300 in 5% milk (1gm dry milk in 20ml TBST) and GAPDH polyclonal antibodies (SANTA CRUZ). Both membranes were hybridized overnight at 4˚C while shaking at constant 30 rpm rotation. Next, the membranes were washed 3 times with TBST for 5 minutes on the shaker before 1:2000 diluted ECL anti-mouse IGg(GE Healthcare) was added to each membrane for incubation for one hour at room temperature on the shaker. The membrane was then washed with TBST 3 times for 5 minutes each. For enhanced chemiluminescence (ECL) detection (GE healthcare), the detection reagents were added to the membranes and allowed to incubate for 5 minutes away from light at room temperature. Lastly, the membrane was transferred to a cassette and developed in the dark room with x-ray films (Thermo Scientific). The films were incubated for 10 to15 minutes before developing in the film-developing machine. The images were finally scanned and quantified with ImageJ (NIH). The experiment was done in triplicates and the target protein band intensity was normalized against GAPDH band.

Quantitative polymerase chain reaction (qPCR)

UM1, UM2, UM5 and UM6 cells were grown in a 10 cm culture dish to 80%-90% confluence. mRNA was collected in two steps; first step was the sample lysis and homogenization, and second step was RNA purification. Quick-RNA Mini prep (ZYMO Research) was used for RNA extraction. The mRNA was converted to cDNA using the Superscriptase III kit (Invitrogen). The mRNA concentration was measured using the Nano-drop analyzer. A 1.5ug of mRNA was converted to cDNA, and the resultant cDNA sample for NHOK, UM1, UM2, UM5 and UM6 cells were measured and all diluted to 100ug/uL. Finally, 1uL of

each cDNA sample was pipetted into a 50uL microentrifuge tube along with 10 uL SYBR Green Super mix 2X, 0.4 uL of a mix of both forward and reverse Hsp90α primers (10 uM), and sterilized water to make a total of 20uL as a final volume. The qPCR was customized with the following 5-cycle settings: denaturation at 94°C for 40 s, annealing at 55°C for 30s, extension at 68°C for 90s for 40 cycles, and a final extension at 68°C for 8 minutes using a CFX96 qPCR instrument (Bio-Rad) . The Cq values were obtained from the CFX96 qPCR instrument and analyzed for fold change using the delta-delta Ct method. The Hsp90α primer used for qPCR listed in **(Table .1)**.

Transient si-Hsp90α transfection

Hsp90α siRNA was used to transiently knock down Hsp90α mRNA expression in UM1 and UM5 HNSCC. bob v bv6-well plate of UM1 and UM5 cell lines were prepared by growing the cells to 80% confluence in 10 cm culture dish. After the cells were washed three times with PBS, trypsin was added to the cells followed with a 5 minute incubation. Subsequently, quenching with a 10 ml complete DMEM supplemented with 10% FBS (Gemini) and 1% Penicillin (Invitrogen) was followed. The cells were then centrifuged at 1500rpm for 5 minutes, resuspended in fresh complete DMEM and homogenized. The cells were counted and transferred to a six well plate at 180,000 cells per well for UM1 and 500,000 cells per well for UM5. The cells were then distributed evenly and transferred carefully for the overnight incubation. The cells were monitored for integrity and growth to reach the 60-70% confluence. On day two, a mix of si Hsp90α or si-Control (SANTA CRUZ), RNAimax (Transfecting reagent), and serum-free DMEM was added to each well after washing with PBS. The cells then incubated in the

CO2 incubator for 8 to 12 hours. Wells were washed from the reagents and Complete DMEM was added. The cells were incubated for additional 48 hours for protein collection.

After 72 hours from the addition of the siRNA, the wells were washed with PBS followed with adding the lysing buffer (Rehydration Buffer). The plate were rocking on ice for 15 minutes. The cells were then scraped and transferred to a labeled 1.5mL micro centrifuge tube to be centrifuged at 14,000 rpm for 5 minutes at 4°C. The lysate was collected and the levels of proteins were quantified using micro BCA assay at 595 nM. The protein lysate was stored in -80C for a subsequent western blotting.

Proliferation assay

Hsp90α was knocked down using siRNA as described above in UM1 and UM5 cell lines. Forty-eight hours after Hsp90α knockdown was completed, the proliferation assay started and be considered Day 1 of the proliferation assay. On Day 1, the complete medium was removed and the cells were washed once with PBS. The cells were lysed with 300uL 0.25% trypsin (Invitrogen) for 5 minutes and quenched with 1.5mL complete media. The culture plates were carefully inspected under a microscope to make sure 100% of the cells were free from the surface. The cells were removed from the wells and counted using the Vi-CELL XR (Cell Viability Analyzer) (Beckman Coulter). The process was followed at 24hr intervals for four days

Wound healing assay

Hsp90α was knocked down using siRNA as described above in UM1 and UM5 cell lines. After the cells reached around 90% confluence, the complete medium was removed and the cells α washed with PBS three times. Using a 200uL sterile pipette, three wounds were made

vertically at thirds across the 6 well plate. The wells were washed with PBS once, and 3 ml of serum-free DMEM was added to each well. Images were obtained at 0hr, 12hr, 18hr and 24hr. At each measurement, the width of the wound was recorded.

Invasion assay

Hsp90α was knocked down using siRNA as described above in UM1 and UM5 cell lines. The cells were washed with PBS, trypsinized with 250uL trypsin, homogenized in serum-free DMED and counted using the Nano drop analyzer. 50,000 cells of each cell group were added to the membranous inserts of the BD BioCoat Matrigel Invasion Chambers. Complete medium was used as the chemoattractant and was added to the wells of the labeled chambers for 22 hours in the incubator. The next day, the medium was removed from the inserts, and the membranes were dried carefully with a Q-Tip. Cells were stained Using the Diff-quick staining kit . Lastly, The cells were photographed using microscope with mounted camera and invading cells were counted.

Mass Spectrometry/ Co-IP

Protein samples (CoIP_UM1, CoIP_UM2, CoIP_UM5, CoIP_UM6 and CoIP_NHOK) were prepared using Dynabeads® M-280 Tosylactivated beads (Invitrogen). Sample contaminants were removed by running SDS-PAGE. We performed in gel trypsin digestion and the resulting peptides were analyzed by LC-MS/MS on Q. Exactive MS. The MS/MS spectra were searched against a UniRef100 human database using a local MASCOT search engine (V.2.3) through the Proteome Discoverer software (V.1.3). Homologous protein

redundancy was reduced by using the Scaffold software. The protein relative abundance was calculated based on spectrum counting.

Co-IP (Co-immunoprecipitation)

UM1 and UM5 were grown in a 10 cm culture plate to 80%-90% confluence, washed 3 times with cold PBS, the cells were lysed on ice with 500uL lysis buffer containing 50mM Tris-base, 150 mM NaCl, 1 mM EDTA, 1% NP-40 and 1X protease inhibitor cocktail (Sigma-Aldrich). The lysate were Collected with scraping and transferred to a 1.5 ml centrifuge tube, centrifuged for 10 minutes at 14,000 G, and the supernatants were collected. Next, 132uL of homogenized Dynabeads® M-280 Tosylactivated beads (Invitrogen)were transferred to each of three labeled tubes; one for SOX11 antibodies, the other tube for an irrelevant IGg and the third without antibodies. the beads were placed on magnet and washed three times with buffer A containing 0.1 M borate at pH 9.5. 10 µg SOX11 Antibodies and irrelevant IGg (SANTA CRUZ) were added each to its labeled tube. 150uL of Buffer A and 100 µl Buffer C (3M ammonium sulphate in Buffer A) were transferred to each tube. the tubes were Incubated on a roller at 37°C for 22 hours.Beads were then placed back on magnet followed with washing three times with buffer A. 1 ml Buffer D containing 0.5% (w/v) BSA in PBS was added to each tube, the tubes were incubated back at 37°C for 1 hour on a roller. Beads were placed back on magnet followed with washing three times with buffer E containing 0.1% (w/v) BSA in PBS. Re-suspend the beads in Buffer E to achieve a final bead Concentration of 20 ug/ul. Protein lysate was added to the beads and incubated at 4C for 48 hrs on a roller. Beads were placed back on magnet followed

with washing three times with buffer E. The supernatant was transferred to new tubes, the beads were eluted using citric acid followed with neutralization with NaOH. Western blotting was used to visualize the protein-protein interaction using Hsp90α Antibodies to detect Hsp90α protein. The Co-IP experiment has been optimized after running the experiment several times using different conditions of the washing time, the ionic strength of the washing buffers and the lysing buffer compositions.

Statistical Analysis

All experiments in this study had been conducted in triplicates. Error bars and standard of deviation were measured. Statistical analysis was performed using Student's t-test to reveal if there is statistically significance difference between two sets of data. A value of $P<0.05$ was considered as statistically significant.

Transient si-SOX11 transfection

si-SOX11 siRNA was used to transiently knock down Hsp90α mRNA expression in UM1 and UM5 HNSCC as described previously.

RESULTS

Differential expression of Hsp90α between high and low invasive HNSCC cells

The western blotting results when quantified using ImageJ as density-quantification tool showed a significant differential expression between the invasive HNSCC (UM1 and UM5) and the low invasive HNSCC (UM2 and UM6). Hsp90α expression in UM1was 2.6 times more than its expression in UM2 ($P<0.05$), whereas, UM5 showed 1.8 hight expression of Hsp90α than UM6 ($P<0.001$) **(Figure. 3)**.

Quantitative polymerase chain reaction (qPCR)

qPCR was used to compare the gene expression (transcriptional activity) of Hsp90α between the high invasive HNSCC (UM1 and UM5) and the low invasive HNSCC (UM2 and UM6). The results mirrored the differential expression of the Hsp90α protein. After standardizing the CT values of Hsp90α of the five tested cell lines (NHOK, UM1, UM2, UM5, UM6) against actin that served as a house-keeping gene, fold change was calculated based on the power of delta delta CT method. The resulted showed that Hsp90α expression in UM2 comprise 38.8% of its expression in UM1 ($P<0.05$). A similar pattern was reflected between UM5 and UM6; where Hsp90α gene expression in UM6 comprise 32.6% of its expression in UM5 ($P<0.05$) **(Figure. 4)**

Knockdown of Hsp90α

To analyze the effect of Hsp90α on the metastatic phenotypic properties of the head and neck cancer, we performed a knockdown Hsp90α using siRNA in UM1 and UM5 cell lines.

Following the knockdown , western blotting was used to confirm the Hsp90α Knock down. A quantification of the western was done using ImageJ software showed around 80% reduction in Hsp90α expression in UM1 ($p<0.01$) **(Figure. 5)**, and 90% reduction in Hsp90α in UM5 ($p<0.01$) when compared to their prospective control groups **(Figure. 6)**

si-RNA knockdown of Hsp90α inhibits the proliferation of UM1 and UM5 cell lines

Over a course of four days, the effect of Hsp90α knockdown in UM1 and UM5 cells on the proliferation rates was investigated. The overall trend shows that Hsp90α knockdown inhibits the proliferation of UM1 **(Figure. 7)** and UM5 **(Figure. 8)** cell lines. Both UM1 and UM5 knockdown groups showed significant decrease in the cell population when compared with the control group ($p<0.05$).

si-RNA knockdown of Hsp90α inhibits on the migration in UM1 and UM5 cell lines

Wound healing assay was preformed to test if knockdown of Hsp90α affects the migration capability of UM1 **(Figure. 9)**. The results indicate that there is significant decrease in migration capability of UM1 after the knockdown with an average of 40% reduction in UM1 migration ($p < 0.001$)

si-RNA knockdown of Hsp90α diminishes on the invasion of UM1 and UM5 cell line

An invasion assay was performed to capture the effect of Hsp90α on the cellular invasion ability of UM1 and UM5 cells. The results show that a significantly decreased number of the invading UM1 (99% reduction) **(Figure. 10)** and UM5 (89.2% reduction) cells after knockdown ($p < 0.001$) **(Figure. 11)**.

Co-IP with MS

MS analysis had shown that Hsp90α is ranked as one of the most abundant proteins pool that bind to SOX11 in the highly invasive UM1 and UM5 as well as the low invasive HNSCC UM2 and UM6 when compared to NHOK, With (UM1/NHOK) ratio as 9.8, (UM5/NHOK) ratio as 8.6, (UM2/NHOK) ratio as 8.4 and (UM6/NHOK) ratio as 7.4 **(Figure. 12).**

Co-IP with Western Blotting

Western blotting of the Co-IP sample confirmed the binding observed in the LC-MS/MS data result between SOX11 and Hsp90α. The results showed the detection of Hsp90α in the SOX11 Co-IP and the whole lysate samples, while, no Hsp90α protein was detected in the negative control sample **(Figure. 13).**

Effect of SOX11 Knockdown on the expression of Hsp90α

To analyze whether SOX11 has a regulatory role on the expression of Hsp90α, we performed a knockdown SOX11 using siRNA in UM1 and UM5 cell lines. Following the knockdown , western blotting followed with the ImageJ was used to visualize and analyze SOX11 and Hsp90α protein expression respectively. We concluded that after the knockdown of SOX11, there wasn't a significant reduction in the expression of Hsp90α. A quantification of the western blotting was done using ImageJ software showed only around 24% reduction in Hsp90α expression in UM1 **(Figure. 14)**, and 25% reduction in Hsp90α in UM5 ($p<0.05$) when compared to their prospective control groups **(Figure. 15)**.

DISCUSSION

We compared the expression levels of Hsp90α between highly invasive and low invasive HNSCC cells. Four cancer cell lines (UM1, UM2, UM5, and UM6) were selected for this study. UM1 and UM2 were initially established from a same cancer patient, with UM1 possessing a more invasive and metastatic ability compared to UM2. Similarly, UM5 cells are more invasive than UM6 cells. Both Western blot and qPCR analyses indicated that Hsp90α is significantly over-expressed in highly invasive cancer cells compared to low invasive cancer cells.

Secondly, in order to demonstrate the functional role of Hsp90α role in HNSCC, siRNA was used to knock down the expression of Hsp90α in highly invasive cancer cell lines UM1 and UM5 and invasion, migration and proliferation assays were performed . The proliferation assay showed that knockdown of Hsp90α inhibited the proliferation of UM1 and UM5 cells, which reflects the proliferation-promotion nature of Hsp90α. The migration assay, similarly, showed Hsp90α knockdown impairs the migration capability of UM1 and UM5 cells when compared to the cells transfected with siRNA control. Lastly, The invasion assay results reflected a well-known effect of Hsp90 in other cancer cell lines, showing a significant decrease in the invasive potential of UM1 and UM5 cells after Hsp90α was knocked down.

Over-expression of Hsp90α chaperone is a common observation that contributes to cancer pathogenesis. The diversity of Hsp90α client proteins leads to its significant effect on key oncogenic signaling leading to increased angiogenesis, anti-apoptotic signals, and survival in cancer micro-environments, making the up-regulated Hsp90α a powerful pro-invasive and pro-

metastatic protein. Based on preliminary datas from our lab, the transcription factor SOX11 is up-regulated in highly invasive HNSCC cell lines, UM1 and UM5, when compared to the low invasive HNSCC cell lines, UM5 and UM6. To identify potential SOX11-interacting proteins, we performed Co-IP to pull down SOX11-binding proteins and then used LC-MS/MS with database searching to identify these proteins. The highly invasive cell lines, UM1 and UM5, had shown highly abundant levels of Hsp90α when compared to NHOKs and low-invasive cell lines, UM2 and UM6. This finding was further confirmed by Co-IP with Western blotting, which indeed suggests functional binding between SOX11 and Hsp90α.

SOX11 as a transcription factor had been associated with different cancer cell lines and is thought to play an important role as an up-stream regulator for many key oncogenic protein expression. In the HNSCC, SOX11 was found to be elevated in the high invasive cancer cell lines, a similar pattern to Hsp90α expression. Based on this study, it can be interpreted that SOX11 may not be a key regulator transcription factor to the Hsp90α gene (heat chock factor).

More experiments are needed to be conducted to further confirm the proposed bio-chemical binding between Hsp90α and SOX11. Finding the role of Hsp90α on nuclear localization, stability, and the levels of SOX11 activity would highly highlight the biological functions of Hsp90α in SOX11 signaling, and suggest that Hsp90α could be an important contributor to elevated SOX11 in head and neck tumors. Next step would be systemically analyzing the different regions of the potential bing between the two proteins, followed with a sire-directed mutagenesis to further confirm the importance of the binding region in the proposed bio-chemical interaction.

CONCLUSION

Our studies have suggested that Hsp90α may play an important functional role in HNSCC, promoting cancer cell proliferation, migration and invasion. Meanwhile, we demonstrated the biochemical binding between SOX11 and Hsp90α, which implies that SOX11 may be a client protein of Hsp90α.

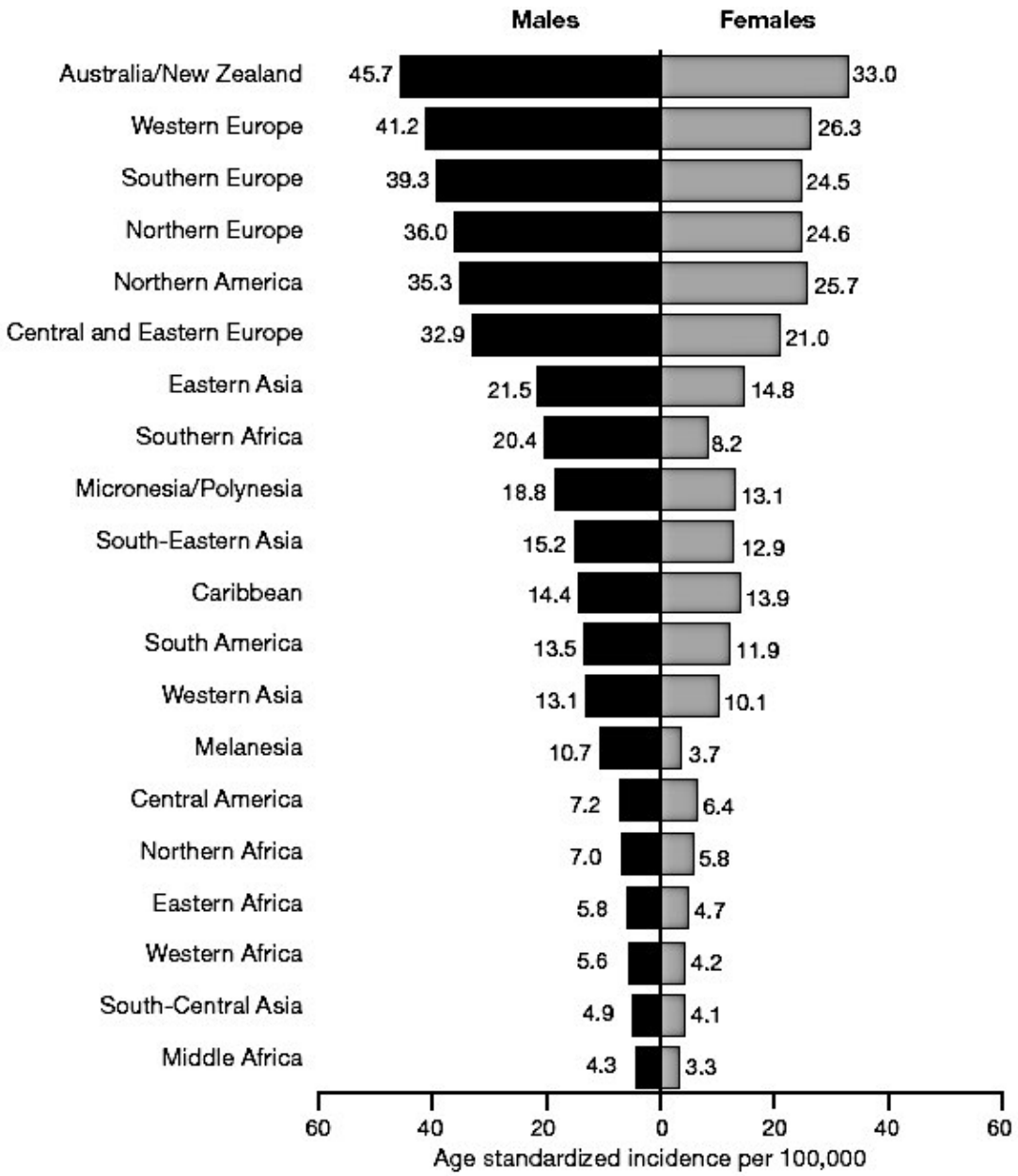

Figure 1. Age standardized incidence rates of oral cancer

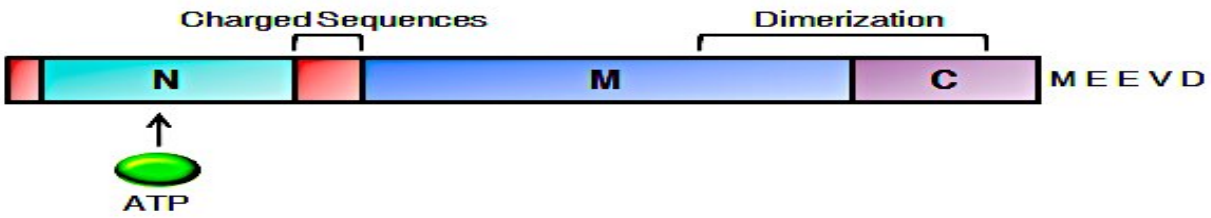

Figure 2. Domains of Hsp90α gene

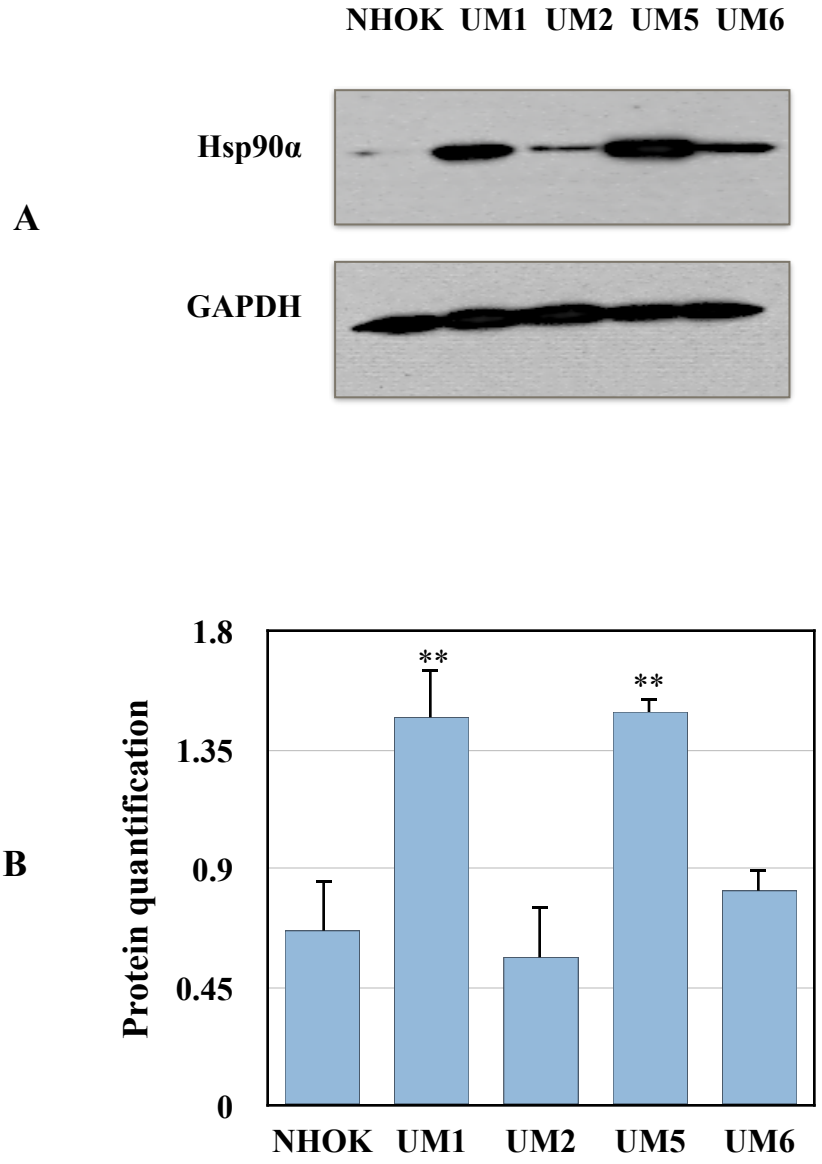

Figure 3. A. Western blot analysis showing the expression level of Hsp90α and GAPDH among UM1, UM2, UM5, UM6 and NHOK. **B.** Quantification of Western blotting results using the ImageJ. With ($p<0.001$) between UM1 and UM2 and between UM5 and UM6 cell lines. (** indicates $p < 0.001$)

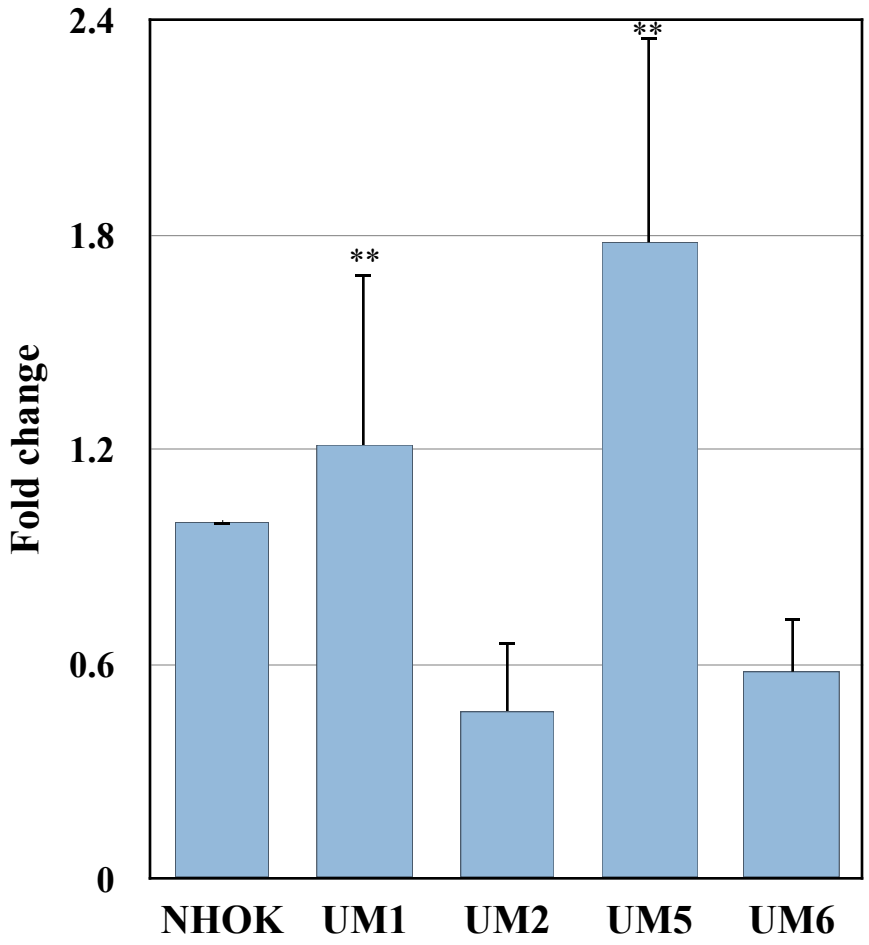

Figure4. qPCR analysis showing expression of Hsp90α in UM1, UM2, UM5, UM6 and NHOK. gene expression of Hsp90α in UM1 and UM5 cells are significantly higher than those in UM2 and UM6 cells. ($p < 0.01$). (** indicates $p < 0.001$)

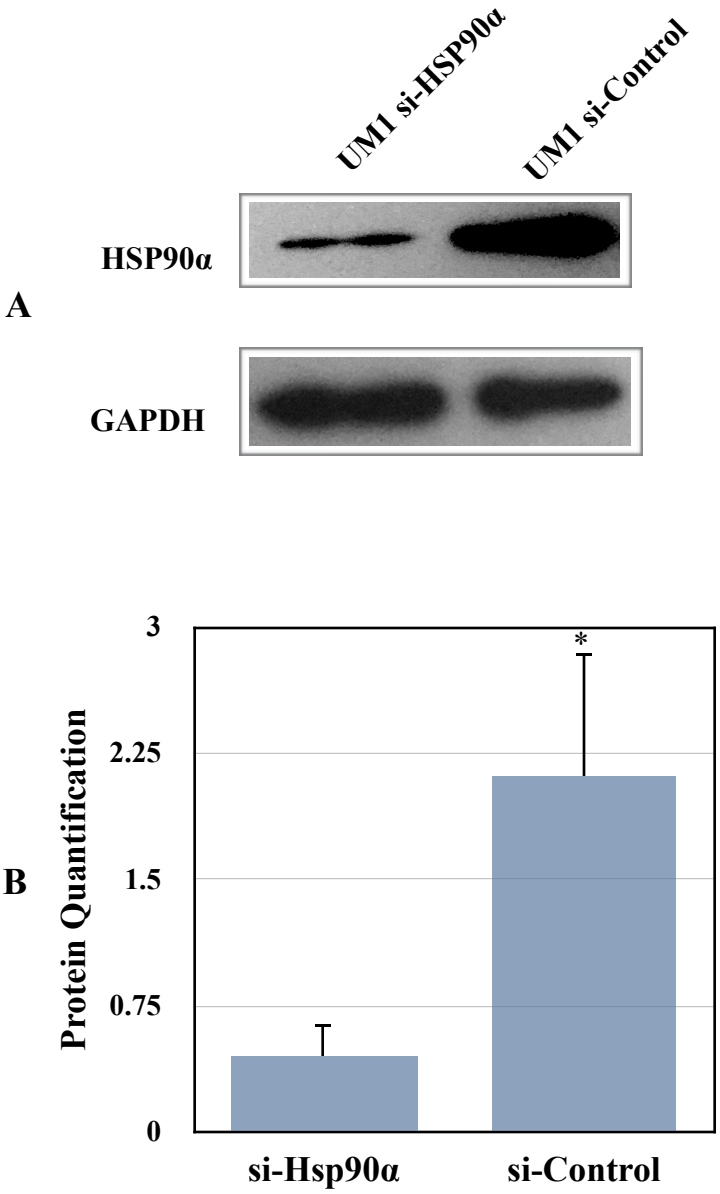

Figure 5. A. Western blot analysis of Hsp90α expression in UM1 following Hsp90 KD. **B.** Quantification of western blotting results using the ImageJ. (* indicates $p < 0.05$).

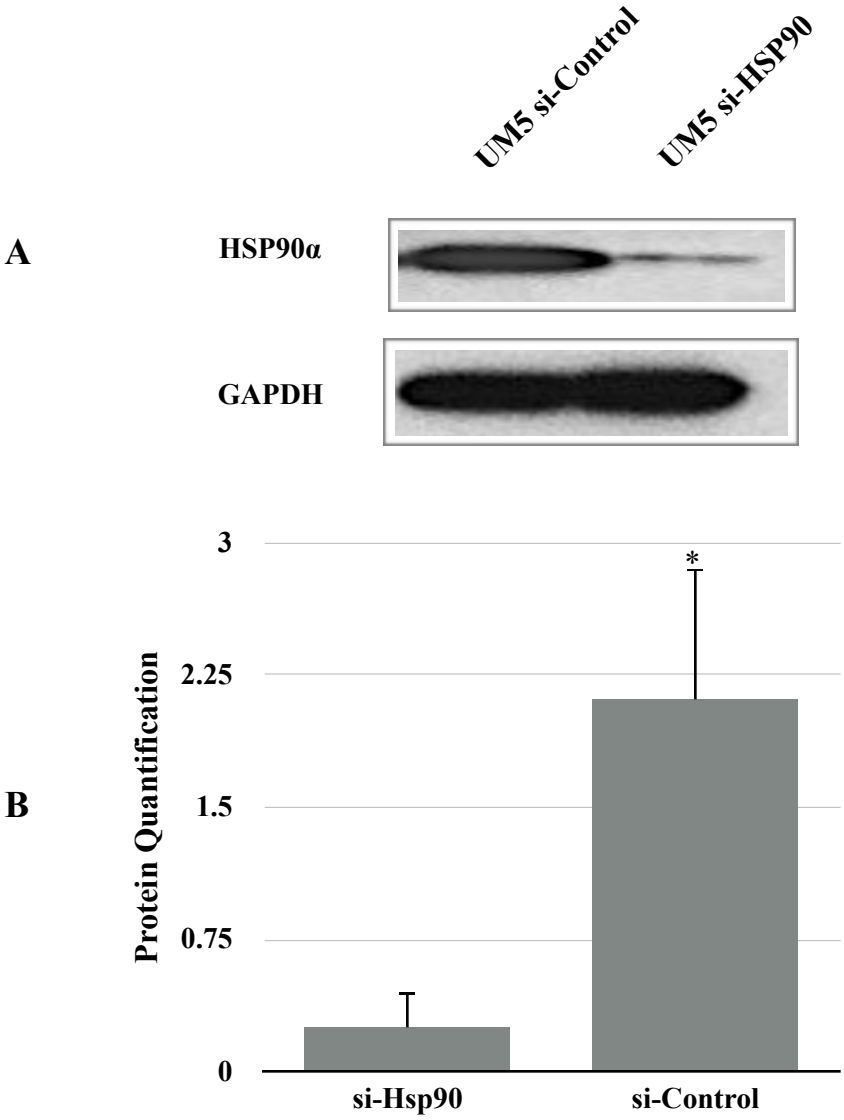

Figure 6. A. Western blot analysis of Hsp90α expression in UM5 following Hsp90 KD. **B.** Quantification of Hsp90α expression using the ImageJ following SOX11 knockdown. (* indicates $p < 0.05$).

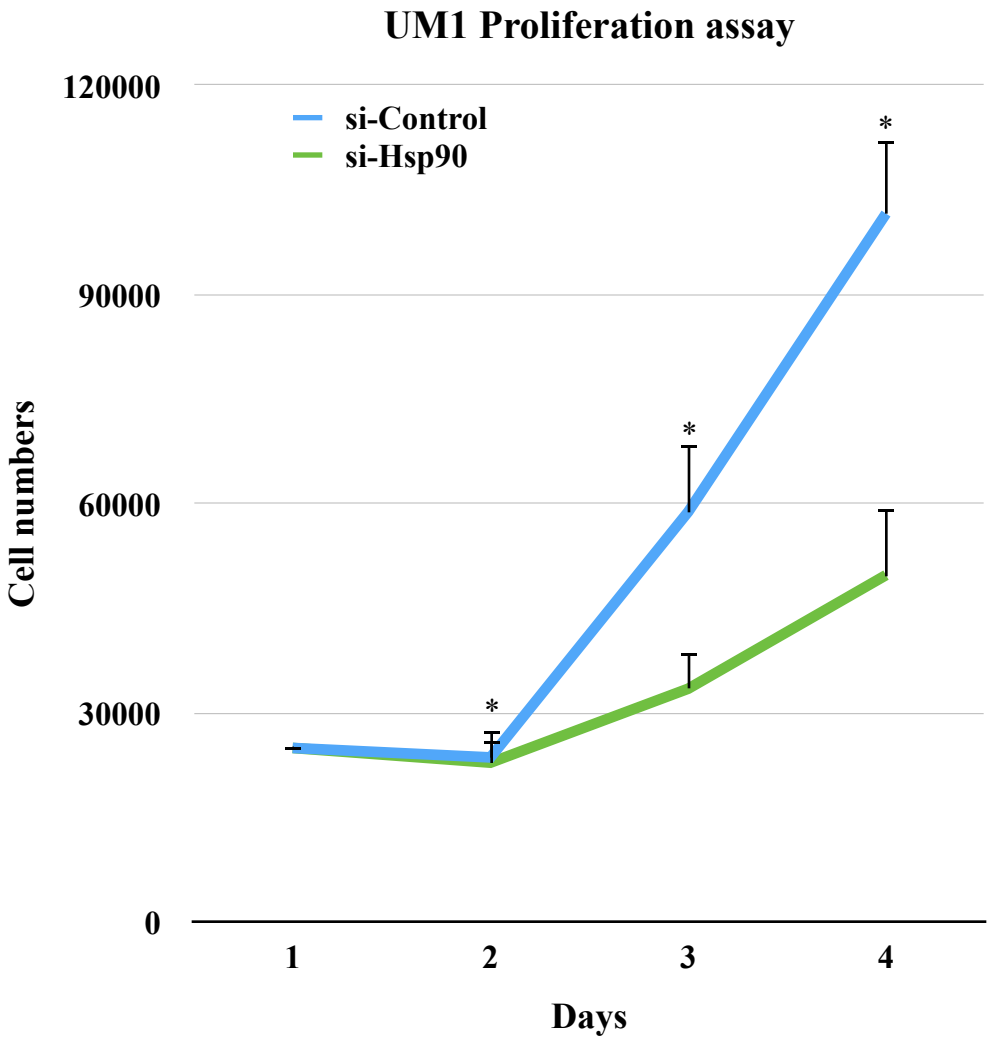

Figure 7. UM1 proliferation assay comparing control and knockdown Hsp90α. Overall trend shows that Hsp90α knockdown has a decreased proliferation in UM1 cells. (* indicates $p < 0.05$)

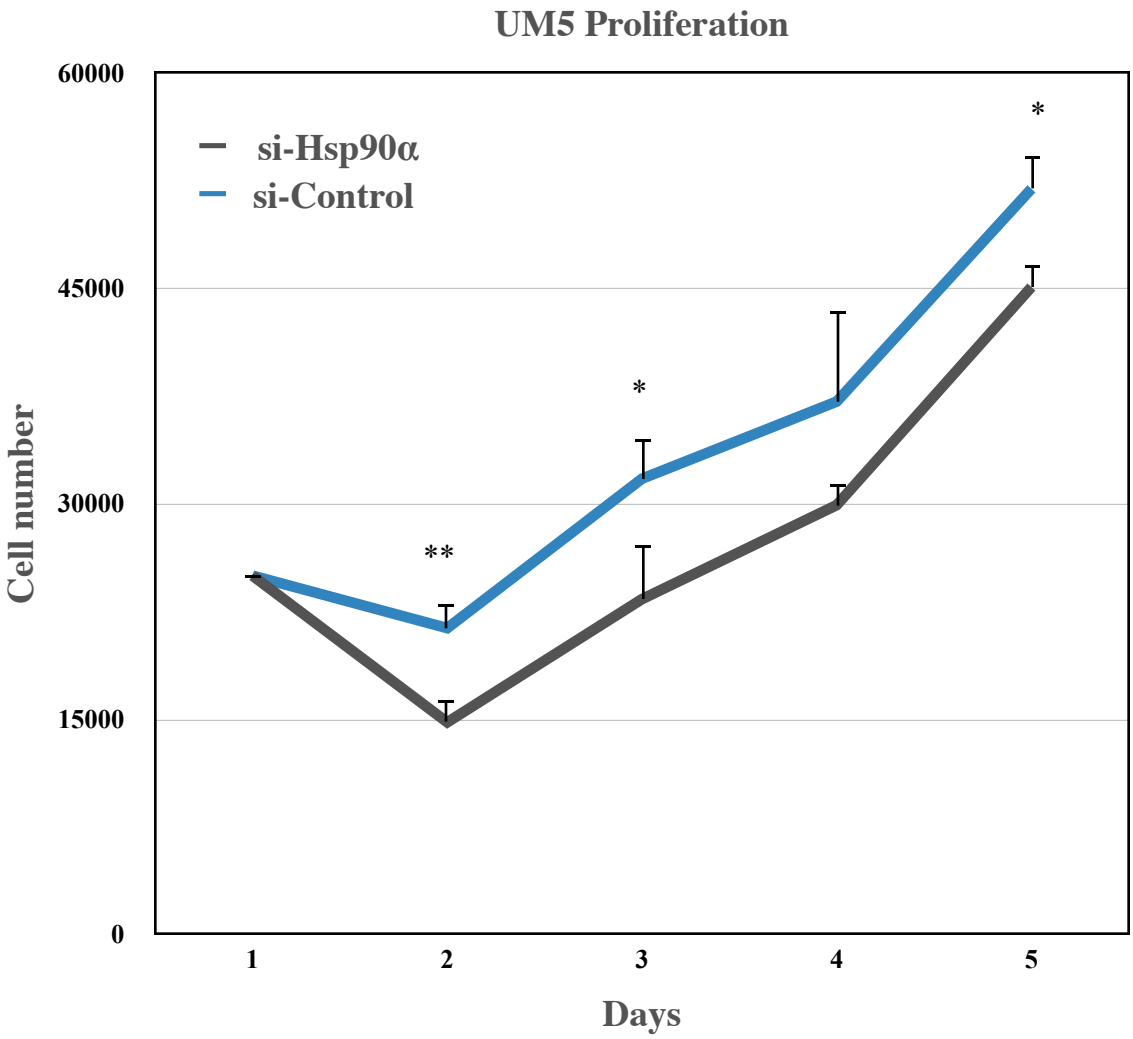

Figure 8. UM5 proliferation assay comparing control and knockdown Hsp90α. Overall trend shows that Hsp90α knockdown has a decreased proliferation in UM5 cell lines. (* indicates $p < 0.05$) (** indicates $p < 0.01$)

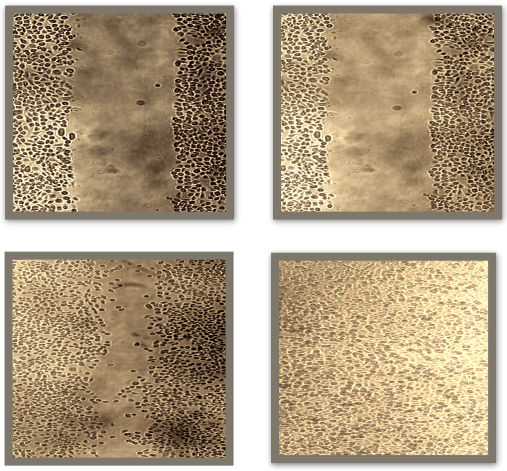

si-Hsp90α si-Control

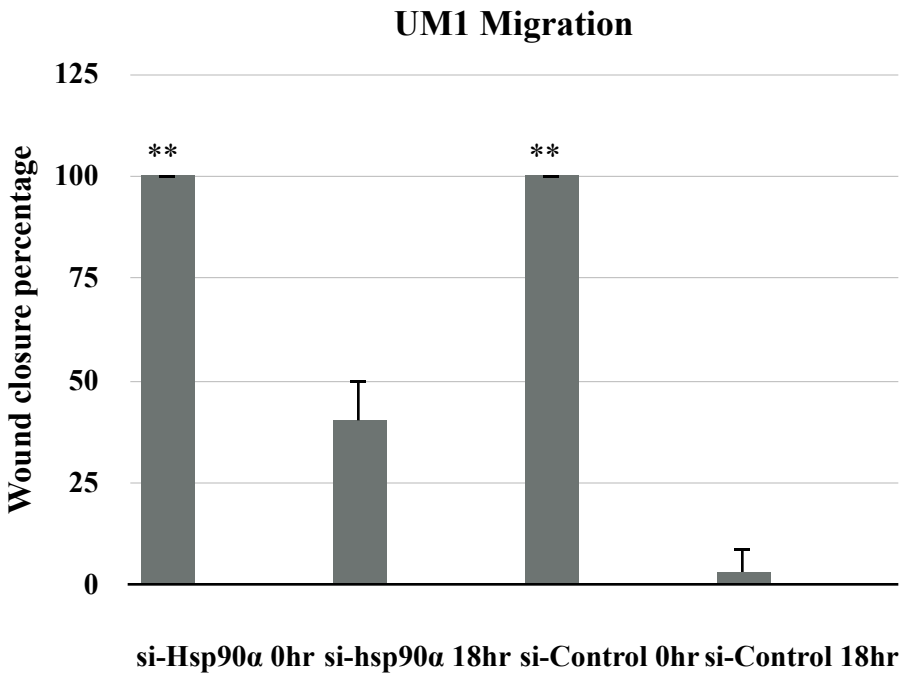

Figure 9. UM1 migration assay comparing control and Hsp90α KD resulted in 40% reduction in the migration ability. (** indicates $p < 0.001$)

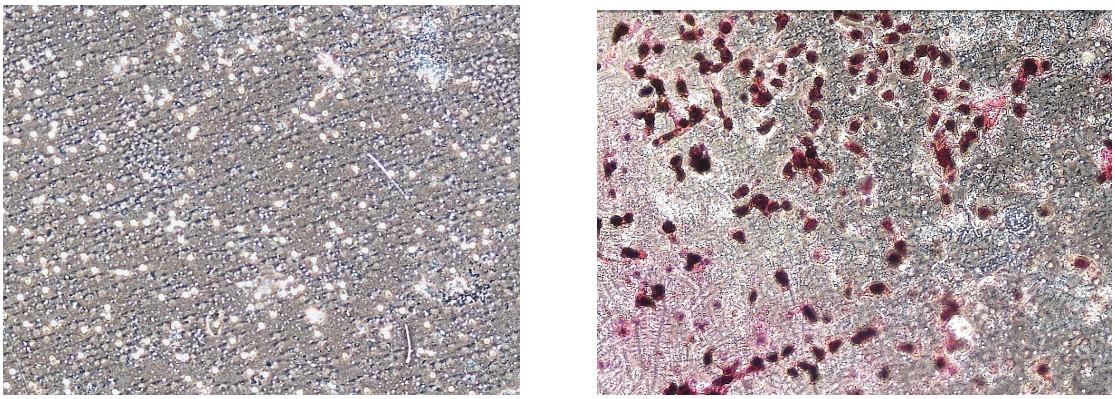

si-Hsp90α si-Control

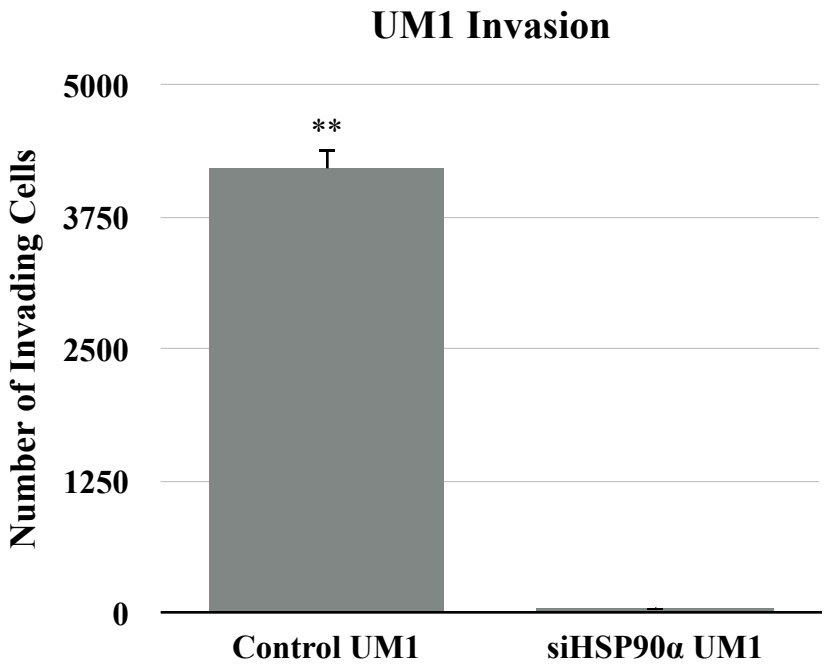

Figure 10. UM1 invasion assays comparing control and knockdown Hsp90α. After siRNA knockdown, UM1 showed a 99% ($p<0.001$) decrease in invasion potential. (** indicates $p < 0.001$)

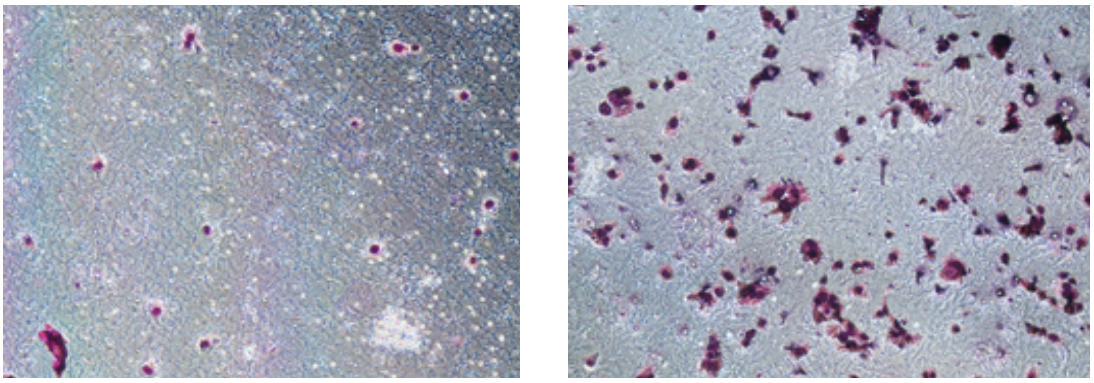

si-Hsp90α si-Control

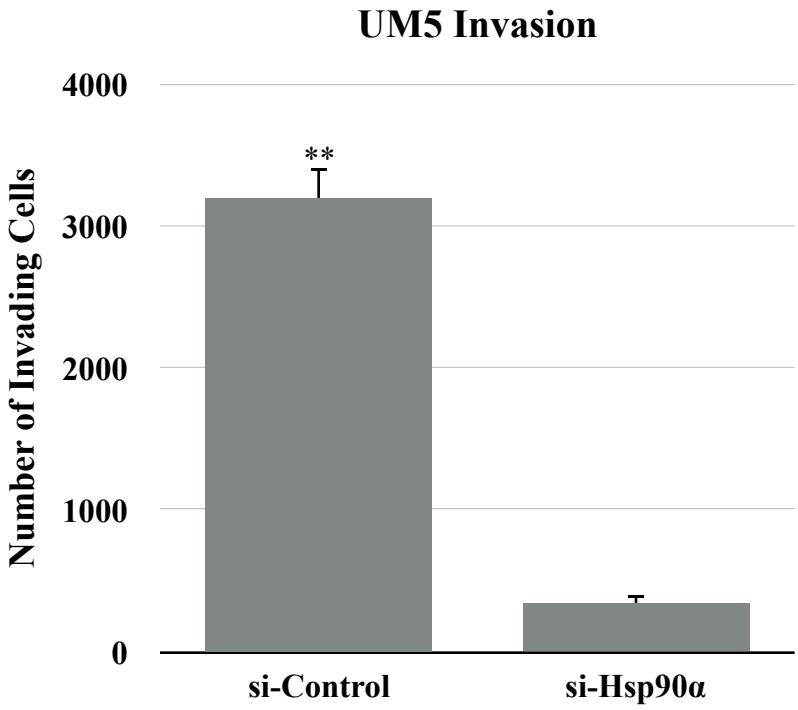

Figure 11. UM5 invasion assays comparing control and knockdown Hsp90α. After siRNA knockdown, UM5 showed a 89.2% ($p<0.001$) decrease in invasion potential. (** indicates $p < 0.001$)

Table 6: Comparison of identified proteins and their relative quantitation in CoIP samples (sorted by ratio 1 (UM1/NHOK)

Identified Proteins (919)	Acc. No.	MW	Spectra counts (NHOK)	Spectra counts (UM1)	Spectra counts (UM2)	Spectra counts (UM5)	Spectra counts (UM6)	Ratio 1 (UM1/NHOK)	Ratio 2 (UM2/NHOK)	Ratio 3 (UM5/NHOK)	Ratio 4 (UM6/NHOK)
cDNA FLJ60647, highly similar to Keratin, type II c	B4DKV4	56 kDa	0	93	62	45	59	94.0	63.0	46.0	60.0
Annexin (Fragment) n=1 Tax=Homo sapiens RepID	H0YM50	28 kDa	0	38	46	0	44	39.0	47.0	1.0	45.0
Full-length cDNA clone CS0DB009YA03 of Neurob	Q86TX4	62 kDa	0	20	61	21	9	21.0	62.0	22.0	10.0
cDNA FLJ58087, highly similar to Alpha-actinin-4 r	B4E337	64 kDa	0	19	64	35	16	20.0	65.0	36.0	17.0
14-3-3 protein beta/alpha n=1 Tax=Homo sapiens	B5BU24	28 kDa	0	19	18	8	17	20.0	19.0	9.0	18.0
Alpha actinin 4 short isoform n=1 Tax=Homo sapi	D6PXK4	80 kDa	0	18	56	40	19	19.0	57.0	41.0	20.0
Plastin-2 n=1 Tax=Homo sapiens RepID=PLSL_HUI	P13796	70 kDa	0	17	19	15	12	18.0	20.0	16.0	13.0
IQ motif containing GTPase activating protein 1 n=	A4QPB0 (+1)	189 kDa	0	16	19	7	6	17.0	20.0	8.0	7.0
Isoform 3 of Exportin-2 n=1 Tax=Homo sapiens Re	P55060-3	108 kDa	0	15	11	4	12	16.0	12.0	5.0	13.0
cDNA FLJ56307, highly similar to Ubiquitin thioest	B4DPD5	35 kDa	0	15	19	3	4	16.0	20.0	4.0	5.0
Cytoskeleton-associated protein 4 n=1 Tax=Homo	Q07065 (+2)	66 kDa	0	15	5	11	6	16.0	6.0	12.0	7.0
cDNA FLJ54090, highly similar to 4F2 cell-surface a	B4E2Z3 (+4)	56 kDa	0	14	11	6	25	15.0	12.0	7.0	26.0
cDNA FLJ76863, highly similar to Homo sapiens st	A8K690	63 kDa	0	13	15	5	14	14.0	16.0	6.0	15.0
Ubiquitin-like modifier-activating enzyme 1 n=2 Ta	P22314	118 kDa	0	12	17	8	3	13.0	18.0	9.0	4.0
Keratin, type II cuticular Hb6 n=1 Tax=Homo sapie	O43790	53 kDa	0	12	0	0	0	13.0	1.0	1.0	1.0
Bleomycin hydrolase (Fragment) n=1 Tax=Homo s	J3KSD8	30 kDa	0	12	3	0	0	13.0	4.0	1.0	1.0
cDNA FLJ56016, highly similar to C-1-tetrahydrofo	B7Z809 (+3)	110 kDa	0	11	9	3	10	12.0	10.0	4.0	11.0
MSN protein (Fragment) n=1 Tax=Homo sapiens R	Q6PJT4	39 kDa	0	11	13	3	0	12.0	14.0	4.0	1.0
Isoform 3 of Myosin-10 n=1 Tax=Homo sapiens Re	P35580-3	231 kDa	0	10	56	159	0	11.0	57.0	160.0	1.0
Protein disulfide-isomerase A4 n=1 Tax=Homo sap	P13667	73 kDa	0	10	9	8	3	11.0	10.0	9.0	4.0
EEF2 protein (Fragment) n=1 Tax=Homo sapiens R	Q6PK56	65 kDa	0	9	12	12	9	10.0	13.0	13.0	10.0
cDNA FLJ56337, highly similar to High mobility gro	B7Z965	20 kDa	0	9	11	2	7	10.0	12.0	3.0	8.0
Protein DJ-1 n=1 Tax=Homo sapiens RepID=K7ELW	K7ELW0	18 kDa	0	9	8	4	3	10.0	9.0	5.0	4.0
cDNA FLJ55325, highly similar to Heat-shock prote	B4DF68 (+2)	86 kDa	0	9	4	7	3	10.0	5.0	8.0	4.0
Annexin n=1 Tax=Homo sapiens RepID=E9PHT9_H	E9PHT9	18 kDa	0	9	14	1	5	10.0	15.0	2.0	6.0
Purine nucleoside phosphorylase n=1 Tax=Homo s	P00491 (+1)	32 kDa	0	9	0	3	0	10.0	1.0	4.0	1.0
Heat shock protein HSP 90-alpha n=6 Tax=Homo s	P07900	85 kDa	4	48	41	42	36	9.8	8.4	8.6	7.4
cDNA FLJ53691 fis, clone BRAWH3018548, highly	B3KUG2	110 kDa	0	8	14	3	3	9.0	13.0	6.0	4.0
Peroxiredoxin-5, mitochondrial n=1 Tax=Homo sa	P30044	22 kDa	0	8	10	2	10	9.0	11.0	3.0	11.0

Figure 12. Comparison of the identified proteins and their relative abundance in Co-IP UM1, UM2, UM5 and UM6 samples (Sorted by their ratio to NHOK)

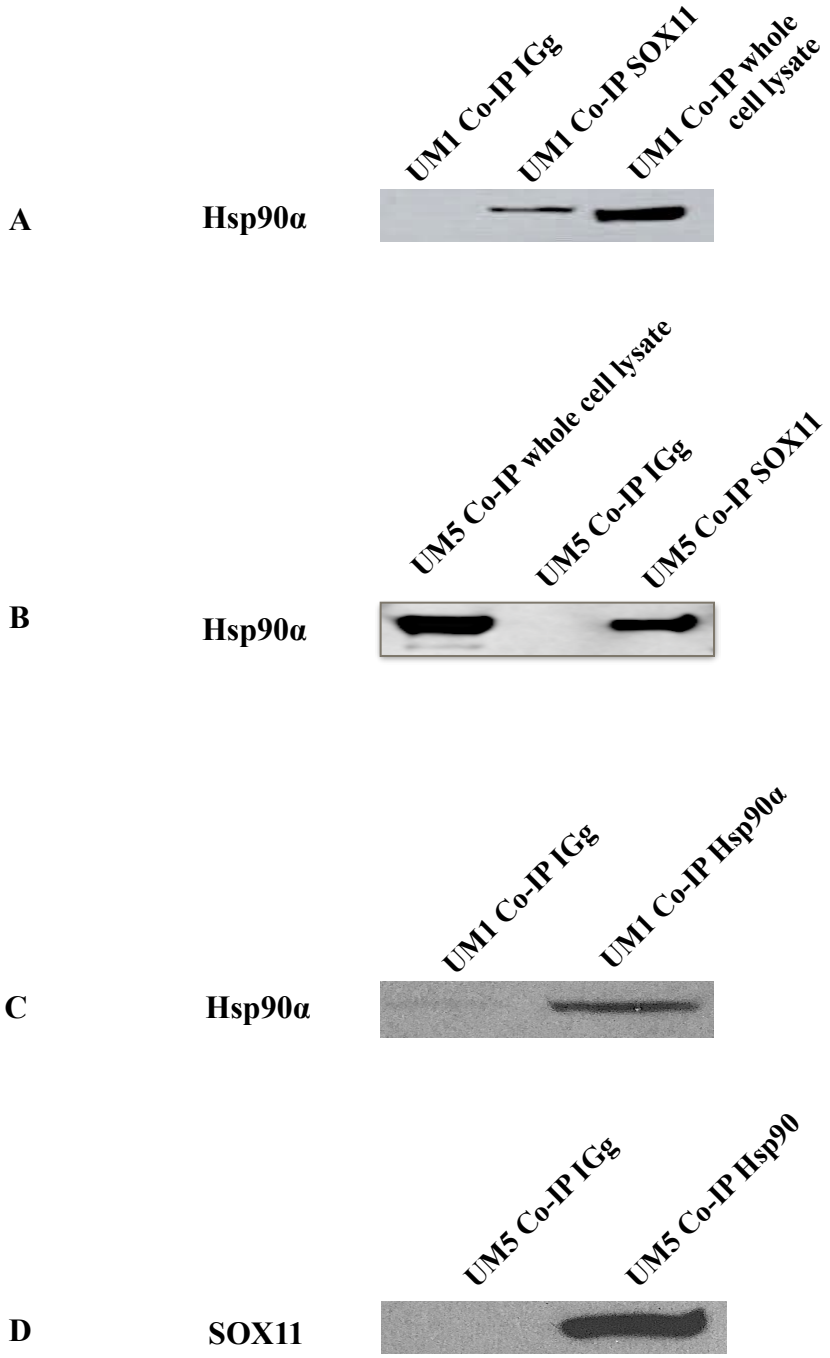

Figure 13. A. Western Blot analysis of UM1 SOX11 Co-IP. **B**. Western Blotting analysis of UM5 SOX11 Co-IP. **C.** Western Blotting analysis of UM1 Hsp90α Co-IP. **D.** Western Blotting analysis of UM1 Hsp90 Co-IP.

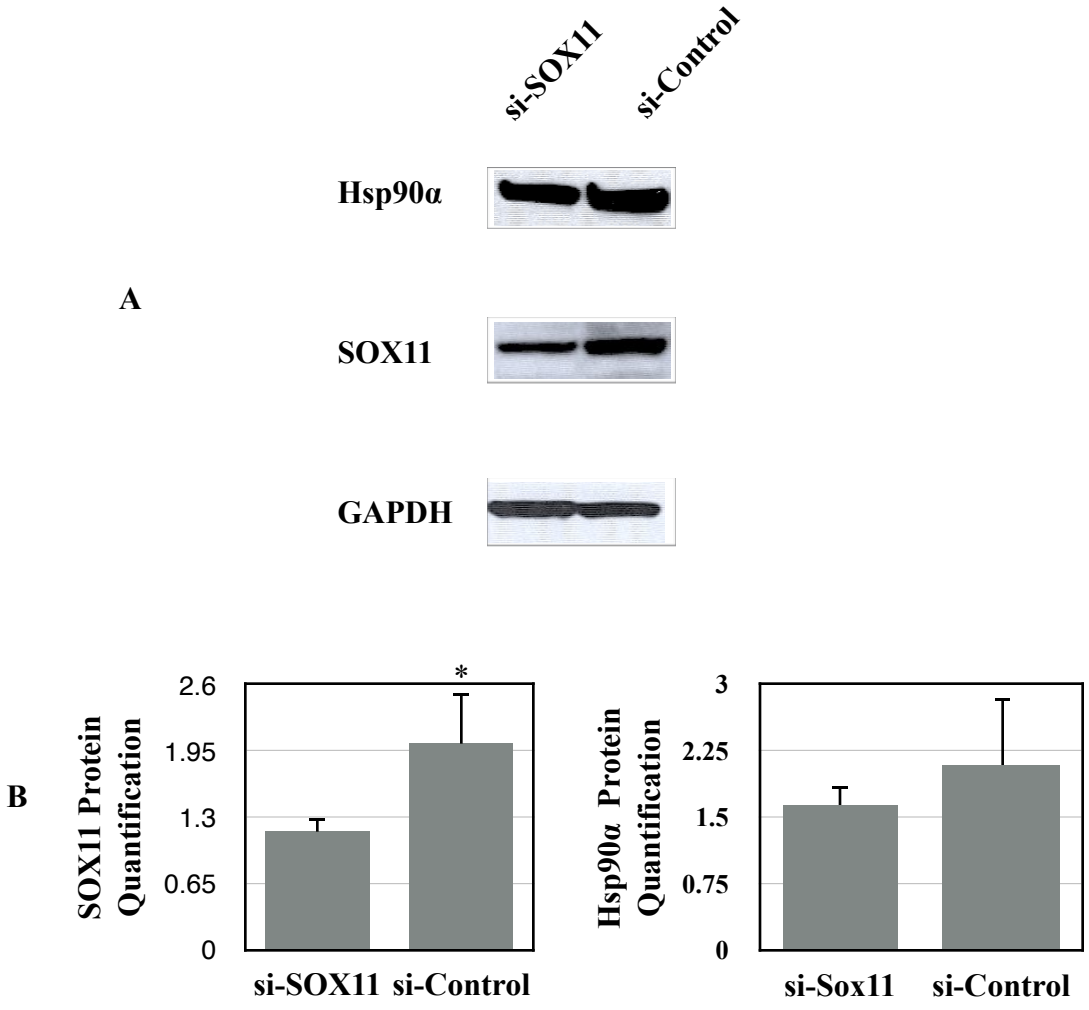

Figure 14 A. Western blotting analysis showing SOX11 and Hsp90α expression following SOX11 KD in UM1 . **B.** Quantification of Hsp90α and SOX11 protein expression using the ImageJ. (* indicates $p < 0.05$)

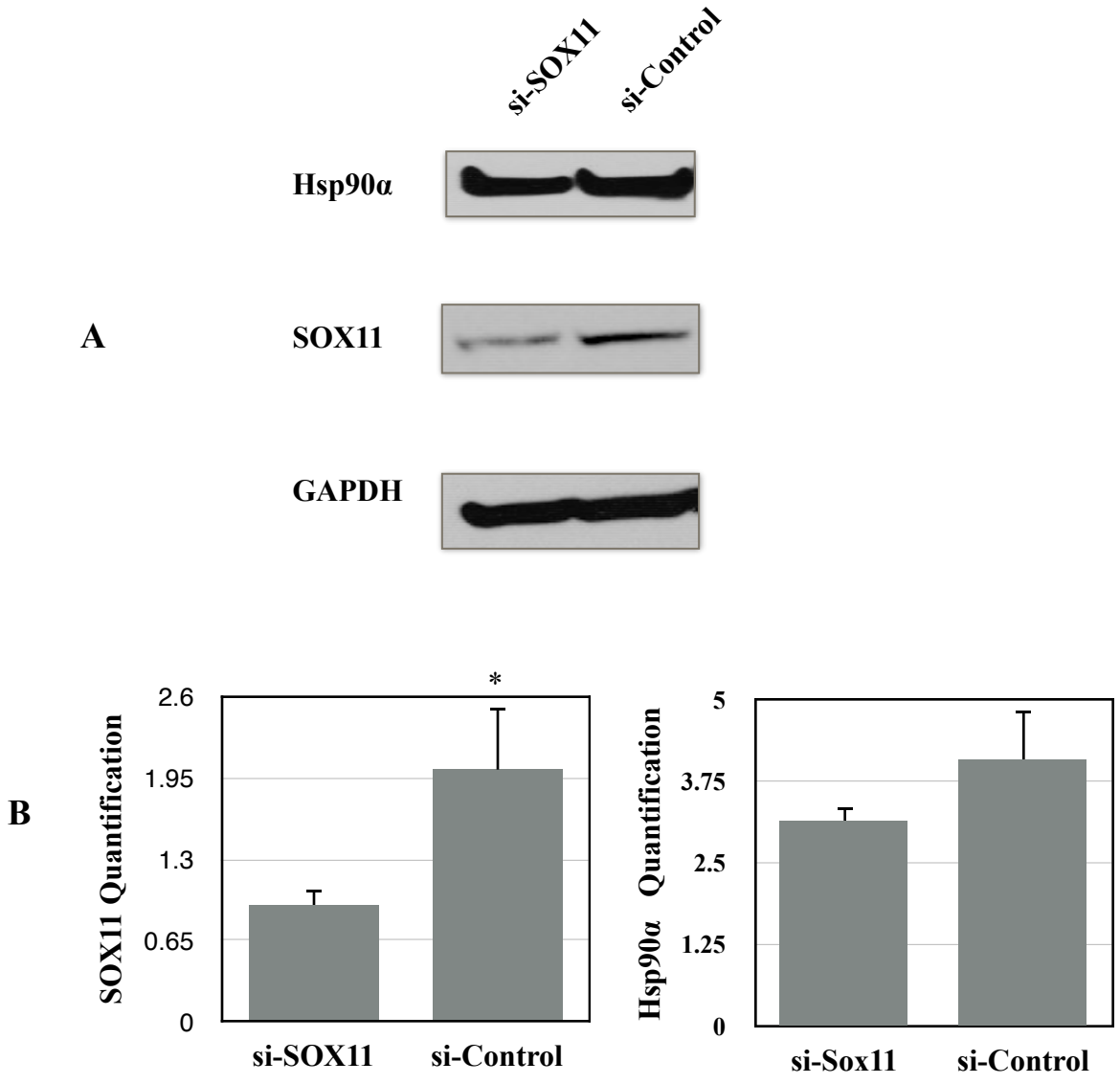

Figure 15. The reduction of the Hsp90α expression in UM5. **A.** Western blotting analysis showing SOX11and Hsp90α expression following SOX11 KD in UM5. **B.** Quantification of Hsp90α and SOX11 protein expression using the ImageJ. (* indicates $p < 0.05$)

Table of Primers

Gene	Forward primer	Reverse primer
Hsp90α promoter	TGGACAGCAAACATGGAGAG	CCAGGTGTTTCTTTGCTGCC

.

REFERENCES

[1] S. M. Rothenberg and L. W. Ellisen, “The molecular pathogenesis of head and neck squamous cell carcinoma.,” *J. Clin. Invest.*, vol. 122, no. 6, pp. 1951–7, 2012.

[2] A. Jemal, F. Bray, M. M. Center, J. Ferlay, E. Ward, and D. Forman, “Global Cancer Statistics: 2011,” *CA. Cancer J. Clin.*, vol. 61, no. 2, pp. 69–90, 2011.

[3] M. Hashibe, P. Brennan, S.-C. Chuang, S. Boccia, X. Castellsague, C. Chen, M. P. Curado, L. Dal Maso, A. W. Daudt, E. Fabianova, L. Fernandez, V. Wünsch-Filho, S. Franceschi, R. B. Hayes, R. Herrero, K. Kelsey, S. Koifman, C. La Vecchia, P. Lazarus, F. Levi, J. J. Lence, D. Mates, E. Matos, A. Menezes, M. D. McClean, J. Muscat, J. Eluf-Neto, A. F. Olshan, M. Purdue, P. Rudnai, S. M. Schwartz, E. Smith, E. M. Sturgis, N. Szeszenia-Dabrowska, R. Talamini, Q. Wei, D. M. Winn, O. Shangina, A. Pilarska, Z.-F. Zhang, G. Ferro, J. Berthiller, and P. Boffetta, “Interaction between tobacco and alcohol use and the risk of head and neck cancer: pooled analysis in the International Head and Neck Cancer Epidemiology Consortium.,” *Cancer Epidemiol. Biomarkers Prev.*, vol. 18, no. 2, pp. 541–550, 2009.

[4] L. Vidal and M. L. Gillison, “Human Papillomavirus in HNSCC: Recognition of a Distinct Disease Type,” *Hematology/Oncology Clinics of North America*, vol. 22, no. 6. pp. 1125–1142, 2008.

[5] K. Cosmopoulos, M. Pegtel, J. Hawkins, H. Moffett, C. Novina, J. Middeldorp, and D. A. Thorley-Lawson, “Comprehensive profiling of Epstein-Barr virus microRNAs in nasopharyngeal carcinoma.,” *J. Virol.*, vol. 83, no. 5, pp. 2357–2367, 2009.

[6] C. R. Leemans, B. J. M. Braakhuis, and R. H. Brakenhoff, “The molecular biology of head and neck cancer.,” *Nat. Rev. Cancer*, vol. 11, no. 1, pp. 9–22, 2011.

[7] F. Ritossa, “A new puffing pattern induced by temperature shock and DNP in drosophila,” *Experientia*, vol. 18, no. 12, pp. 571–573, 1962.

[8] F. U. Hartl, “Molecular chaperones in cellular protein folding.,” *Nature*, vol. 381, no. 6583, pp. 571–579, 1996.

[9] S. D. Westerheide and R. I. Morimoto, “Heat shock response modulators as therapeutic tools for diseases of protein conformation,” *Journal of Biological Chemistry*, vol. 280, no. 39. pp. 33097–33100, 2005.

[10] R. I. Morimoto, M. P. Kline, D. N. Bimston, and J. J. Cotto, “The heat-shock response: regulation and function of heat-shock proteins and molecular chaperones.,” *Essays Biochem.*, vol. 32, pp. 17–29, 1997.

[11] Y. Li, T. Zhang, S. J. Schwartz, and D. Sun, “New developments in Hsp90α inhibitors as anti-cancer therapeutics: Mechanisms, clinical perspective and more potential,” *Drug Resist. Updat.*, vol. 12, no. 1–2, pp. 17–27, 2009.

[12] S. F. Falsone, B. Gesslbauer, F. Tirk, A.-M. Piccinini, and A. J. Kungl, “A proteomic snapshot of the human heat shock protein 90 interactome.,” *FEBS Lett.*, vol. 579, no. 28, pp. 6350–6354, 2005.

[13] A. J. McClellan, Y. Xia, A. M. Deutschbauer, R. W. Davis, M. Gerstein, and J. Frydman, “Diverse Cellular Functions of the Hsp90α Molecular Chaperone Uncovered Using Systems Approaches,” *Cell*, vol. 131, no. 1, pp. 121–135, 2007.

[14] R. Zhao, M. Davey, Y. C. Hsu, P. Kaplanek, A. Tong, A. B. Parsons, N. Krogan, G. Cagney, D. Mai, J. Greenblatt, C. Boone, A. Emili, and W. A. Houry, “Navigating the chaperone network: An integrative map of physical and genetic interactions mediated by the Hsp90α chaperone,” *Cell*, vol. 120, no. 5, pp. 715–727, 2005.

[15] K. A. Borkovich, F. W. Farrelly, D. B. Finkelstein, J. Taulien, and S. Lindquist, “hsp82 is an essential protein that is required in higher concentrations for growth of cells at higher temperatures.,” *Mol. Cell. Biol.*, vol. 9, no. 9, pp. 3919–3930, 1989.

[16] C. Didelot, D. Lanneau, M. Brunet, A.-L. Joly, A. De Thonel, G. Chiosis, and C. Garrido, “Anti-cancer therapeutic approaches based on intracellular and extracellular heat shock proteins.,” *Curr. Med. Chem.*, vol. 14, no. 27, pp. 2839–2847, 2007.

[17] L. H. Pearl and C. Prodromou, “Structure and mechanism of the Hsp90α molecular chaperone machinery.,” *Annu. Rev. Biochem.*, vol. 75, pp. 271–294, 2006.

[18] K. Richter, J. Soroka, L. Skalniak, A. Leskovar, M. Hessling, J. Reinstein, and J. Buchner, "Conserved conformational changes in the ATPase cycle of human Hsp90α," *J. Biol. Chem.*, vol. 283, no. 26, pp. 17757–17765, 2008.

[19] S. K. Wandinger, K. Richter, and J. Buchner, "The Hsp90α chaperone machinery," *Journal of Biological Chemistry*, vol. 283, no. 27. pp. 18473–18477, 2008.

[20] E. G. Mimnaugh, C. Chavany, and L. Neckers, "Polyubiquitination and proteasomal degradation of the p185(c-erbB-2) receptor protein-tyrosine kinase induced by geldanamycin," *J. Biol. Chem.*, vol. 271, no. 37, pp. 22796–22801, 1996.

[21] G. P. Nagaraju, T.-E. Long, W. Park, J. C. Landry, L. Taliaferro-Smith, A. B. Farris, R. Diaz, and B. F. El-Rayes, "Heat shock protein 90 promotes epithelial to mesenchymal transition, invasion, and migration in colorectal cancer.," *Mol. Carcinog.*, 2014.

[22] A. Ahsan, S. G. Ramanand, C. Whitehead, S. M. Hiniker, A. Rehemtulla, W. B. Pratt, S. Jolly, C. Gouveia, K. Truong, C. Van Waes, D. Ray, T. S. Lawrence, and M. K. Nyati, "Wild-type EGFR is stabilized by direct interaction with Hsp90α in cancer cells and tumors.," *Neoplasia*, vol. 14, no. 8, pp. 670–7, 2012.

[23] B. K. Eustace, T. Sakurai, J. K. Stewart, D. Yimlamai, C. Unger, C. Zehetmeier, B. Lain, C. Torella, S. W. Henning, G. Beste, B. T. Scroggins, L. Neckers, L. L. Ilag, and D. G. Jay, "Functional proteomic screens reveal an essential extracellular role for Hsp90α alpha in cancer cell invasiveness.," *Nat. Cell Biol.*, vol. 6, no. 6, pp. 507–514, 2004.

[24] K. Sidera and E. Patsavoudi, "Extracellular Hsp90α. Conquering the cell surface," *Cell Cycle*, vol. 7, no. 11. pp. 1564–1568, 2008.

[25] J. C. Kiefer, "Back to basics: Sox genes," *Developmental Dynamics*, vol. 236, no. 8. pp. 2356–2361, 2007.

[26] Y. Wang, L. Lin, H. Lai, L. F. Parada, and L. Lei, "Transcription factor Sox11 is essential for both embryonic and adult neurogenesis," *Dev. Dyn.*, vol. 242, no. 6, pp. 638–653, 2013.

[27] B. Weigle, R. Ebner, A. Temme, S. Schwind, M. Schmitz, A. Kiessling, M. A. Rieger, G. Schackert, H. K. Schackert, and E. P. Rieber, “Highly specific overexpression of the transcription factor SOX11 in human malignant gliomas,” *Oncol. Rep.*, vol. 13, no. 1, pp. 139–144, 2005.

[28] Y. Qu, C. Zhou, J. Zhang, Q. Cai, J. Li, T. Du, Z. Zhu, X. Cui, and B. Liu, “The metastasis suppressor SOX11 is an independent prognostic factor for improved survival in gastric cancer,” *Int. J. Oncol.*, vol. 44, no. 5, pp. 1512–1520, 2014.

[29] X. Wang, A. C. Asplund, A. Porwit, J. Flygare, C. I. E. Smith, B. Christensson, and B. Sander, “The subcellular Sox11 distribution pattern identifies subsets of mantle cell lymphoma: Correlation to overall survival,” *Br. J. Haematol.*, vol. 143, no. 2, pp. 248–252, 2008.

[30] S. Sernbo, E. Gustavsson, D. J. Brennan, W. M. Gallagher, E. Rexhepaj, F. Rydnert, K. Jirström, C. A. Borrebaeck, and S. Ek, “The tumour suppressor SOX11 is associated with improved survival among high grade epithelial ovarian cancers and is regulated by reversible promoter methylation,” *BMC Cancer*, vol. 11, no. 1. p. 405, 2011.